ISSN 1001-0742
CN 11-2629/X

2012

Volume 24
Number 8

JOURNAL OF ENVIRONMENTAL SCIENCES

ELSEVIER
Science Press

Sponsored by
Research Center for Eco-Environmental Sciences
Chinese Academy of Sciences

JOURNAL OF ENVIRONMENTAL SCIENCES

(http://www.jesc.ac.cn)

Aims and scope

Journal of Environmental Sciences is an international academic journal supervised by Research Center for Eco-Environmental Sciences, Chinese Academy of Sciences. The journal publishes original, peer-reviewed innovative research and valuable findings in environmental sciences. The types of articles published are research article, critical review, rapid communications, and special issues.

The scope of the journal embraces the treatment processes for natural groundwater, municipal, agricultural and industrial water and wastewaters; physical and chemical methods for limitation of pollutants emission into the atmospheric environment; chemical and biological and phytoremediation of contaminated soil; fate and transport of pollutants in environments; toxicological effects of terrorist chemical release on the natural environment and human health; development of environmental catalysts and materials.

For subscription to electronic edition

Elsevier is responsible for subscription of the journal. Please subscribe to the journal via http://www.elsevier.com/locate/jes.

For subscription to print edition

China: Please contact the customer service, Science Press, 16 Donghuangchenggen North Street, Beijing 100717, China. Tel: +86-10-64017032; E-mail: journal@mail.sciencep.com, or the local post office throughout China (domestic postcode: 2-580).

Outside China: Please order the journal from the Elsevier Customer Service Department at the Regional Sales Office nearest you.

Submission declaration

Submission of an article implies that the work described has not been published previously (except in the form of an abstract or as part of a published lecture or academic thesis), that it is not under consideration for publication elsewhere. The submission should be approved by all authors and tacitly or explicitly by the responsible authorities where the work was carried out. If the manuscript accepted, it will not be published elsewhere in the same form, in English or in any other language, including electronically without the written consent of the copyright-holder.

Submission declaration

Submission of the work described has not been published previously (except in the form of an abstract or as part of a published lecture or academic thesis), that it is not under consideration for publication elsewhere. The publication should be approved by all authors and tacitly or explicitly by the responsible authorities where the work was carried out. If the manuscript accepted, it will not be published elsewhere in the same form, in English or in any other language, including electronically without the written consent of the copyright-holder.

Editorial

Authors should submit manuscript online at http://www.jesc.ac.cn. In case of queries, please contact editorial office, Tel: +86-10-62920553, E-mail: jesc@263.net, jesc@rcees.ac.cn. Instruction to authors is available at http://www.jesc.ac.cn.

Copyright

ISSN 1001–0742 **Journal of Environmental Sciences** Vol. 24 No. 8 2012

CONTENTS

Serial parameter: CN 11-2629/X*1989*m*184*en*P*24*2012-8

Available online at www.sciencedirect.com
ScienceDirect
Journal of Environmental Sciences 2012, 24(8) 1525–1532
JOURNAL OF ENVIRONMENTAL SCIENCES
ISSN 1001-0742
CN 11-2629/X
www.jesc.ac.cn

Adsorption of mixed cationic-nonionic surfactant and its effect on bentonite structure

Yaxin Zhang[1], Yan Zhao[1,2], Yong Zhu[1], Huayong Wu[1], Hongtao Wang[1,*], Wenjing Lu[1]

1. School of Environment, Tsinghua University, Beijing 100084, China. E-mail: zhangyx08@mails.tsinghua.edu.cn
2. School of Environment, Beijing Normal University, Beijing 100875, China

Received 15 October 2011; revised 14 December 2011; accepted 16 December 2011

Abstract

The adsorption of cationic-nonionic mixed surfactant onto bentonite and its effect on bentonite structure were investigated. The objective was to improve the understanding of surfactant behavior on clay mineral for its possible use in remediation technologies of soil and groundwater contaminated by toxic organic compounds. The cationic surfactant used was hexadecylpyridinium bromide (HDPB), and the nonionic surfactant was Triton X-100 (TX100). Adsorption of TX100 was enhanced significantly by the addition of HDPB, but this enhancement decreased with an increase in the fraction of the cationic surfactant. Part of HDPB was replaced by TX100 which decreased the adsorption of HDPB. However, the total adsorbed amount of the mixed surfactant was still increased substantially, indicating the synergistic effect between the cationic and nonionic surfactants. The surfactant-modified bentonite was characterized by Brunauer-Emmett-Teller specific surface area measurement, Fourier transform infrared spectroscopy, and thermogravimetric-derivative thermogravimetric/differential thermal analyses. Surfactant intercalation was found to decrease the bentonite specific surface area, pore volume, and surface roughness and irregularities, as calculated by nitrogen adsorption-desorption isotherms. The co-adsorption of the cationic and nonionic surfactants increased the ordering conformation of the adsorbed surfactants on bentonite, but decreased the thermal stability of the organobentonite system.

Key words: surfactant; bentonite; surfactant modification; adsorption

DOI: 10.1016/S1001-0742(11)60950-9

Introduction

The remediation of hydrophobic organic contaminants (HOCs) in soil and groundwater has become a key global issue (Rodríguez-Cruz et al., 2008; Shu et al., 2010). Due to their abundance in nature, low cost, easy availability, and high ion exchange capacity, clay minerals have been a suitable choice for the removal of organic pollutants from water (Zhou and Zhu, 2005). However, the negative surface charge of most natural aluminosilicate clay minerals resulted from isomorphous substitutions gives them a comparatively hydrophilic surface that hinders the adsorption of hydrophobic organic pollutants (Senturk et al., 2009). The introduction of long-chain organic surfactant compounds by cation exchange reactions and van der Waals interactions can modify substantially the surface properties of natural clays and endow them with significant hydrophobic characteristics (Chang et al., 2009) and higher organic content for the adsorption of toxicants through partitioning. Surfactant-modified clay mineral, namely, the organoclay, can create an adsorption zone to intercept a contaminant plume and retain the flow of pollutants. Therefore, it can be used as a clay barrier for *in situ* remediation of contaminated aquifers and as a landfill liner for the reduction of HOC leaks (Rodríguez-Cruz et al., 2007; Wang et al., 2010).

The mixtures of different ionic types of surfactants exhibit different properties compared with the corresponding single surfactants, and often cause synergistic/antagonistic effects in both liquid and solid-liquid system (Chu and So, 2001; Sehgal et al., 2009; Zheng and Obbard, 2002). The non-ideal mixing effects in mixed aggregates, which are due to the insertion of head groups between different surfactants, can be ascribed as the main cause of this synergism (Sehgal et al., 2009). These non-ideal mixing effects reduce the electrostatic repulsion between the cationic surfactant head groups, resulting in substantially lower critical micellization concentrations (CMC) compared with individual surfactants (Varade and Bahadur, 2005). Generally, a mixture of nonionic and ionic surfactants increases the stability of the bulk solution, the size of the mixed micelles, as well as their solubilizing capability for HOCs. The unique properties of the surfactant mixture can be favorable in pollutants retention during the utilization of clay.

As reported previously, the adsorbed cationic-nonionic surfactant mixture can enhance the retention of HOCs compared with individual surfactants (Zhao et al., 2010).

* Corresponding author. E-mail: htwang@tsinghua.edu.cn

The clay-sorbed surfactant molecules can be a more effective adsorbent for HOCs (Laha et al., 2009). Moreover, the distribution of HOCs in soil and clay minerals is mainly controlled by their partitioning into organic matter. Higher adsorption of surfactants gives clay higher organic content and hence, higher distribution coefficient of HOCs on organoclay. As a result of which, an understanding of sorptive mechanisms of surfactants is of significant importance. However, there is still a lack of studies on the adsorption of surfactant mixtures on clay minerals. The adsorption of two different solutes can be additive, cooperative, or competitive (Torn et al., 2003). Previous studies on the adsorptive behavior of ionic-nonionic surfactants were mostly carried out with alumina (Somasundaran and Huang, 2000; Zhang and Somasundaran, 2006) and silica (Portet-Koltalo et al., 2001; Thibaut et al., 2000). The results of these studies showed that nonionic molecules intercalate among ionic monomer head groups in the cationic micelles and micelle-like aggregates on the clay surface, thereby producing different antagonistic and synergistic effects. However, alumina and silica are positively charged in neutral pH, which limits their full representation of the normally negatively charged clay and clay minerals. Furthermore, these previous studies mentioned were not aimed at increasing the adsorption capability of clay minerals, let alone applying them to HOC remediation. Therefore, an examination of the mechanisms on the adsorption of mixed surfactant onto clay mineral is needed.

Surfactant adsorption causes structural changes on adsorbents such as soil and clay minerals. Surfactant species and interlayer arrangement affect the pore structure, surface properties, and adsorptive behavior of surfactant-modified adsorbents (Wang et al., 2004). The microtopography of single surfactant-modified clay minerals has been studied widely using Brunauer-Emmett-Teller (BET), a measurement method of surface area (Zhu et al., 2009), Fourier transform infrared (FT-IR) spectroscopy (Erdem et al., 2010), thermogravimetric-derivative thermogravimetric/differential thermal analyses (TG-DTG/DTA) (Xi et al., 2010), and transmission electron microscopy and scanning electron microscopy (Senturk et al., 2009). The results of these studies showed that not only surface structural variations but also system stability changes are induced by adsorbed surfactants. However, to the best of our knowledge, structural analyses of clay minerals with adsorbed mixed surfactants have not been conducted extensively. An examination of the structural changes of organoclay is necessary to elucidate surfactant adsorptive mechanisms further.

In the present study, the co-adsorption of the cationic-nonionic surfactant onto bentonite was investigated. Being the most extensively used clay mineral given its advantages of abundance, low cost, and easy availability, limited information has been reported on the adsorptive behaviors of cationic-nonionic surfactant mixtures on bentonite. BET specific surface area measurement, FT-IR spectroscopy, and G-DTG/DTA were used for the structural characterizations of the surfactant modifications and for elucidation of the co-adsorptive mechanisms involved.

1 Material and methods

1.1 Materials

The clay used in this study was bentonite from Shandong Province in China. Triton X-100 (TX100), a nonionic surfactant with a critical micellization concentration (CMC) of about 120 mg/L (0.24 mmol/L) (Sánchez-Martín et al., 2008), was supplied by Pharmacia (USA). 1-Hexadecylpyridinium bromide (HDPB), a cationic surfactant with a CMC value of about 273.6 mg/L (0.68 mmol/L), was purchased from Alfa Aesar (USA). Pentachlorophenol (PCP) was purchased from Dima (USA). The two surfactants and PCP were used as received.

1.2 Adsorption experiments and surfactant analysis

Batch experiments were conducted to determine the surfactant sorption isotherms onto clay mineral using centrifuge tubes (CNW, 40 mL) with Teflon-lined screw caps. The 0.10 g of bentonite and 20.0 mL of an aqueous solution of known surfactant concentration were injected into each tube. The surfactant solution (mixture or single) was set with fixed HDPB concentrations (0, 2, 4, 6, and 8 times of CMC) and different TX100 concentrations (0–3840 mg/L). The tubes were allowed to reach equilibrium at (25 ± 1)°C in a reciprocating shaker for 24 hr, which was proven to be sufficient for the procedure (Sánchez-Martín et al., 2008). The solution and solid phase were then separated by centrifugation at 3000 r/min for 30 min. An appropriate aliquot (about 1.5 mL) of the supernatant was removed and analyzed for TX100 and HDPB concentration using high performance liquid chromatography (HPLC, Agilent 1260, USA) fitted with an ultraviolet (UV) detector and Agilent TC-C18 column (4.5 mm × 250 mm, 5-Micron), with methanol-water (80:20) as the mobile phase at a flow rate of 1.00 mL/min. Chromatography was performed at 35°C. The UV wavelengths were set at 280 and 254 nm for TX100 and HDPB, respectively. Data are shown as the means of two replicates with a deviation of ±5%.

1.3 Characterization of organobentonite

In the current study, the BET specific surface area, pore volume, pore diameter, and fractal dimension of the original and surfactant-modified bentonite were calculated from nitrogen adsorption-desorption isotherms performed on a Quantachrome gas adsorption instrument (Autosorb AS-1 N2). The samples were outgassed for 16 hr at 105°C before the measurements.

FT-IR spectra were obtained on a spectrometer (Spectrum GX, PerkinElmer, USA) in the 4000–400 cm^{-1} region at 4 cm^{-1} resolution. About 2 mg of the milled sample was ground up with 200 mg (FT-IR grade) KBr and compressed into a pellet under vacuum at the pressure of 75 kN/cm^2 for 3 min. Thirty-two scans were performed, averaged for each spectrum, and corrected against air as background on each acquisition.

Analysis using the TG-DTG/DTA was performed through a TGA/DSC (Mettler Toledo, Switzerland) 1 star system (range: 30–900°C) under static air atmosphere at a

heating rate of 10°C/min (gas flow: 100 mL/min containing 21% ± 1% oxygen and 79% ± 1% nitrogen.

2 Results and discussion

2.1 Adsorption of HDPB and TX100 on bentonite

The adsorption isotherms of TX100 in the complete range of concentration used (0–3840 mg/L) under different HDPB concentrations are shown in Fig. 1. The sorption isotherms of TX100 were nonlinear with and without HDPB addition. The cationic surfactant caused a significant increase in the adsorption amount of TX100. With the addition of cationic surfactant (within the concentration of 2–8CMC used), the adsorption amount of TX100 decreased with an increase in HDPB fraction in the mixed surfactant solution.

The adsorption isotherm of pure TX100 on bentonite corresponded with the H-type classification of Giles et al. (1960), with a total adsorption of TX100 at the initial stage. This result indicated the high affinity between the surfactant and the mineral surface. At sub-CMC concentration, TX100 in the bulk solution and solid-water interface existed in monomeric forms. In this region, a monolayer or bilayer of the adsorbed surfactant occurred on the solid surface through ion-dipole-type interaction or hydrogen bond. With the concentration higher than the elevated CMC (CMC_{eff}), the surfactant monomers self-aggregated into micelles in the bulk solution and were not adsorbed onto the clay mineral, hence, the adsorption isotherm reached to the "plateau" region (Liu et al., 1992).

The adsorption isotherms of TX100 with the addition of HDPB showed the increased affinity for TX100. Bentonite is negatively charged because of isomorphic substitution, hence, the cationic surfactants can be adsorbed on bentonite themselves due to electrostatic interaction and through replacement of the inorganic exchangeable cations with layer silicate clays (Xu and Boyd, 1995). The electrostatic attraction for the adsorption of cationic molecules is usually stronger than hydrogen bonding (Zhang and Somasundaran, 2006), therefore HDPB generally adsorbs more than TX100 at the initial stage. The cationic surfactant caused a significant increase in the amount of TX100 adsorbed, indicating a strong synergy between HDPB and TX100. The adsorbed amount of TX100 reached up to 253.5 mg/g in the 2CMC case under an initial concentration of 3840 mg/L, more than twice that without HDPB (115.0 mg/g). The pre-adsorbed HDPB molecules acted as anchors on the bentonite surface, and the adsorbed HDPB formed mixed aggregates with TX100 through chain-chain interactions, thereby promoting TX100 adsorption. At an HDPB concentration higher than 2CMC, the amount of TX100 adsorbed decreased with an increase in HDPB concentration. The mixture of surfactants can decrease the CMC value in the bulk solution effectively; hence, the mixed surfactant concentration needed for micellization decreased as the HDPB concentration increased.

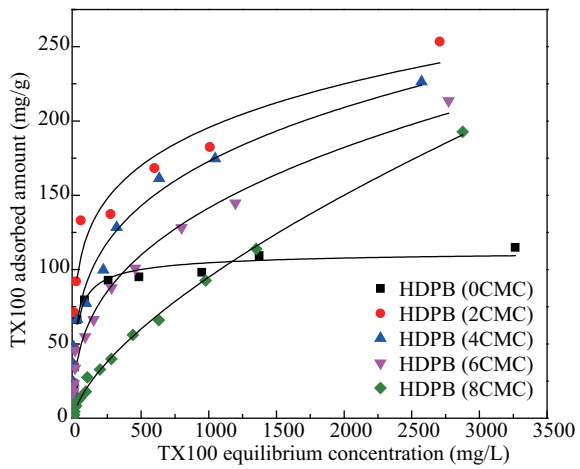

Fig. 1 Adsorption isotherms of TX100 on bentonite with different HDPB concentrations.

The TX100 adsorption isotherms obtained were fitted to the linearized form of Langmuir ($R^2 \geqslant 0.9440$, $p < 0.001$) and Freundlich models ($R^2 \geqslant 0.8782$, $p < 0.001$) as the following Eqs. (1) and (2), respectively:

Langmuir:

$$\frac{C_e}{q} = \frac{C_e}{K_1} + \frac{1}{K_1 K_2} \quad (1)$$

Freundlich:

$$\log q = \log K_f + h_f \log C_e \quad (2)$$

where, C_e (mg/L) is the equilibrium concentration of adsorbate, q (mg/g) is the adsorbed amount per unit mass of clay, K_f (L/kg) and n_f denote the monolayer sorption capacity and sorption constant, respectively, K_1 (mg/g) indicates the maximum adsorption capacity of the surfactant onto clay, and K_2 (L/mg) is an index of adsorption energy. The values of all parameters for the adsorption of TX100 on bentonite at 25°C are included in Table 1. The value of K_f ranged from 1.29 to 47.08 L/kg, with the highest value corresponding to the HDPB 2CMC case. The values of $1/n$ were very low (0.196–0.621), indicating a favorable adsorption over the entire range of the surfactant concentration investigated. In the Langmuir model, the K_1 values ranged from 113.6 to 263.2 mg/g. The highest value of K_1 also corresponded to the HDPB 2CMC case. Both the Langmuir and Freundlich models gave high correlation coefficients to all adsorption curves. The value of K_f and K_1 indicated that with HDPB 2CMC, adsorption of surfactants showed maximized synergistic effect between HDPB and TX100.

As shown in Fig. 2, the adsorbed amount of HDPB decreased linearly with the increased concentration of TX100 in the bulk solution, suggesting that HDPB was "washed out" by TX100. The adsorbed cationic molecules were partially replaced by nonionic molecules at the solid/liquid interface. As indicated by the slope in Fig. 2, the higher original HDPB concentration showed a higher "desorption" rate. Higher HDPB concentration there is in the bulk solution, easier it gets for the formation of mixed micelles that do not adsorb on clay surface. The mixed micelles were comparatively more stable, and competed with the admicelle on the solid/liquid surface for HDPB molecules. Hence, with the increase of TX100 concentration, more

Table 1 Freundlich and Langmuir model parameters for the adsorption of TX100 on bentonite at 25°C

HDPB concentration	Freundlich model			Langmuir model		
	K_f	$1/n$	R^2	K_1	K_2	R^2
0CMC	26.41	0.196	0.8782	113.6	0.032	0.9976
2CMC	47.09	0.207	0.9305	263.2	0.005	0.9743
4CMC	23.22	0.290	0.9465	232.6	0.005	0.9786
6CMC	13.60	0.334	0.9905	227.3	0.003	0.9440
8CMC	1.293	0.621	0.9858	204.1	0.001	0.9502

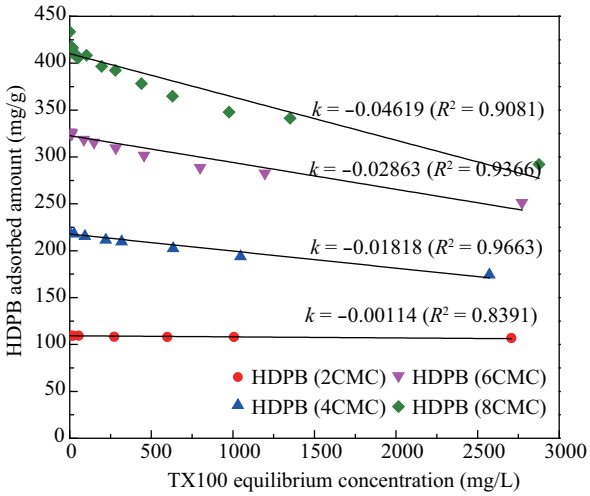

Fig. 2 Adsorbed amount of HDPB on bentonite with different TX100 concentrations. *k* slope of each fitted line.

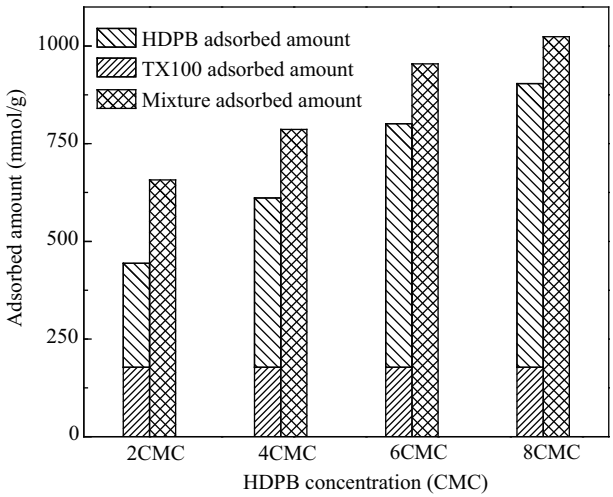

Fig. 3 Summed and mixture adsorption amount of surfactants.

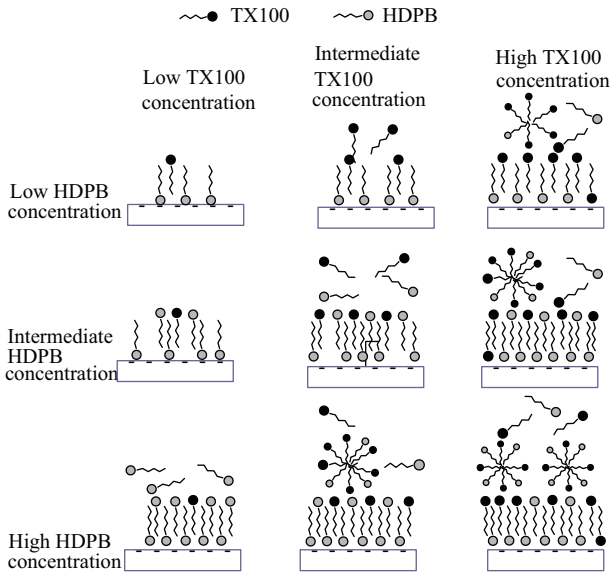

Fig. 4 Adsorption models for TX100/HDPB mixtures on bentonite surface.

HDPB molecules tended to be replaced into the bulk solution.

The calculated adsorption amount of TX100 (with initial concentration of 3840 mg/L) and HDPB (2, 4, 6, 8CMC) alone was compared with the real adsorption amount of TX100/HDPB mixture under the same initial concentration, as shown in Fig. 3. The mixture adsorption amount showed significant increase as compared to the summed results. The adsorption amount of TX100 alone was 177.7 mmol/g, and that of HDPB (2CMC) alone was 265.8 mmol/g, making the total added amount of 443.5 mmol/g. However, with TX100/HDPB mixture, the real adsorption amount reached up to 657.3 mmol/g. This phenomenon can be ascribed to the synergism between cationic and nonionic surfactants, which reinforced their adsorption on clay mineral.

Based on these results, a schematic diagram is proposed in Fig. 4 for the adsorption of TX100/HDPB mixed surfactants on bentonite. At lower concentrations, both surfactants were adsorbed on clay surface through electrostatic interaction and hydrogen bonding, and cationic surfactant was adsorbed more than nonionic surfactant. At intermediate concentrations, HDPB molecules acted as anchors and more TX100 was adsorbed through hydrophobic chain-chain reaction, and formed the mixed aggregates at solid/liquid interface. At higher concentrations, mixed micelles were formed in bulk solution, and adsorption started to reach the plateau.

2.2 BET specific surface areas (SSAs)

The SSA of the surfactant-adsorbed bentonite was determined by the BET method using adsorption data, whereas pore volume and pore size distribution were examined using the Barrett-Joyner-Halenda model based on desorption isotherms. Figure 5 shows the adsorption-desorption isotherms and the corresponding pore size distribution curves (insert) of the original and organobentonite (C_{HDPB} = 4CMC). Non-polar adsorptives such as N_2 do not penetrate into the interlayer regions of well-outgassed Na- or Ca-montmorillonite (Zhu et al., 2009). Therefore, the internal surface area of montmorillonite cannot be detected. Type IV isotherms were displayed (Sing et al., 1985), and a large uptake can be observed at close to saturation pressure, reflecting the capillary condensation in

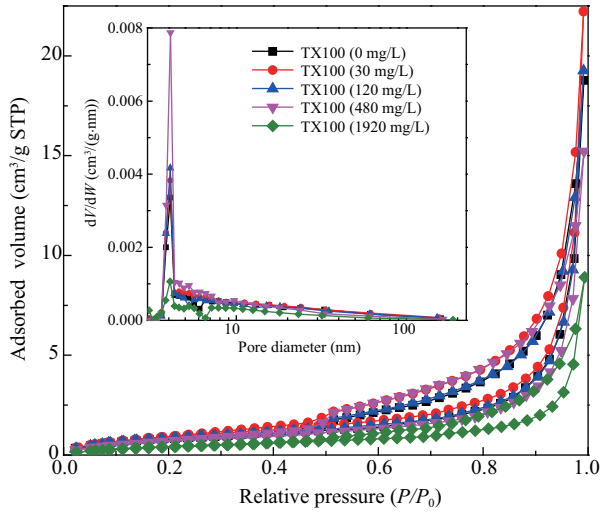

Fig. 5 Nitrogen adsorption-desorption isotherm and pore size distribution curve (insert) of original and organobentonite.

the large pores (Zhu et al., 2009).

As shown in Table 2, compared with untreated bentonite, the SSA of the organic bentonite was very small. The SSA decreased from 28.66 m^2/g for original bentonite to 1.76 m^2/g for organobentonite with the highest surfactant loading level. A similar trend can also be found in the total pore volume as it decreased from 0.072 to 0.014 mL/g. The SSA and pore volume decreased as the amount of loaded surfactant increased. This phenomenon can be attributed to that the intercalated surfactant molecules blocked the passage of N_2 (Juang et al., 2008). Only part of the interlamellar porosity was accessible. On the other hand, a slight increase in pore diameter can be found with surfactant-modified bentonite, because the surfactants can block part of the micropores, causing the average pore size to distribute to larger mesopore proportions.

Another approach that can provide additional information on organobentonite structure in terms of "roughness exponent" is the surface fractal dimension (D). Fractal dimension describes the topography of the real surface based on fractal geometry. This factor is usually between 2 (smooth surface) and 3 (rough surface). The complex pore and surface structure can be well described by fractal dimensions. As nitrogen molecules have difficulty penetrating the interlayer space of clay mineral, fractal dimension D reflects the external surface characterization. Fractal dimension D is derived using the Frenkel-Halsey-Hill (FHH) and Neimark-Kiselev (NK) (Zhu et al., 2009) methods as shown in Table 2. Both D_F and D_N of organobentonite were smaller than those of raw bentonite because the external surface and the jagged edge of clay were covered by surfactant molecules that created a smoother surface. However, co-adsorption of the two different surfactants slightly increased the D value as compared with HDPB 4CMC alone. The reason for this phenomenon can be the competitive effect of TX100 and HDPB on adsorbing sites or the coexistence of micropores and mesopores induced by the organic cation exchange process (Zhu et al., 2009).

2.3 FT-IR spectra

The FT-IR spectra of original bentonite, TX100/bentonite, and HDPB/TX100/bentonite are shown in Fig. 6, in which the concentration of TX100 is fixed at 1920 mg/L. As can be seen from the IR spectra of original bentonite, the absorption peaks at 3625 and 3426 cm^{-1} were due to stretching vibration of H–O–H (Alkaram et al., 2009; Koyuncu et al., 2011). The peak at around 1637 cm^{-1} corresponded to the OH^- deformation of water (Erdem et al., 2010). The band at 1035 cm^{-1} was assigned to the symmetric stretching vibration of Si–O–Si of bentonite (Alkaram et al., 2009), whereas the bands from 720 to 839 cm^{-1} showed the property of quartz (Alkaram et al., 2009). For organobentonite, the CH_2 bending vibration (1468 cm^{-1}) and CH_3-N^+ vibration (1489 cm^{-1}) of the HDPB head group (Ninness et al., 2002) can be attributed to the replacement of interlayer metallic cations by HDPB. The presence of a higher frequency shoulder at 1095 cm^{-1} for Si–O stretching vibration (Singhal and Datta, 2007) suggested the intercalation of surfactant molecules between silica layers.

The bands at around 2918 and 2850 cm^{-1} corresponded to the asymmetric and symmetric stretching frequencies of the CH_2 of the hydrocarbon tails of the surfactants; the changes in these bands can be used to characterize the adsorption of surfactants. The decrease in gauche/trans conformer ratio, namely, the ordering of methylene chains, can be detected by the decrease in frequencies of CH_2 stretching bands (Scheuing and Weers, 1990). As shown in Fig. 6, TX100/bentonite showed CH_2 stretching peaks at significantly higher frequencies (2932 and 2878 cm^{-1}) compared with the HDPB-modified bentonite (around 2918 and 2850 cm^{-1}). The lower frequencies in HDPB/TX100/bentonite revealed the trans conformation of the micelle-like aggregates because of hydrophobic chain-chain reactions and the non-ideal inter-

Table 2 Effects of surfactants on the specific surface areas, pore volume, average pore diameters, and fractal dimension of bentonite[a]

Sample	BET surface area (m^2/g)	Total pore volume (mL/g)	Pore diameter (nm)	Fractal dimension[b]			
				D_N	R^2	D_F	R^2
Bentonite	28.66	0.072	3.81	2.675	0.998	2.666	0.999
TX100 (0 mg/L)	3.04	0.030	4.08	2.510	0.981	2.386	0.998
TX100 (30 mg/L)	3.62	0.036	4.08	2.506	0.989	2.395	0.998
TX100 (120 mg/L)	3.19	0.031	4.09	2.472	0.992	2.411	0.998
TX100 (480 mg/L)	2.80	0.026	4.09	2.534	0.989	2.407	0.999
TX100 (1920 mg/L)	1.76	0.014	4.07	2.532	0.990	2.447	0.998

[a] HDPB concentration was 4CMC.
[b] Fractal dimension (D) is derived using the Frenkel-Halsey-Hill (D_F) and Neimark-Kiselev (D_N).

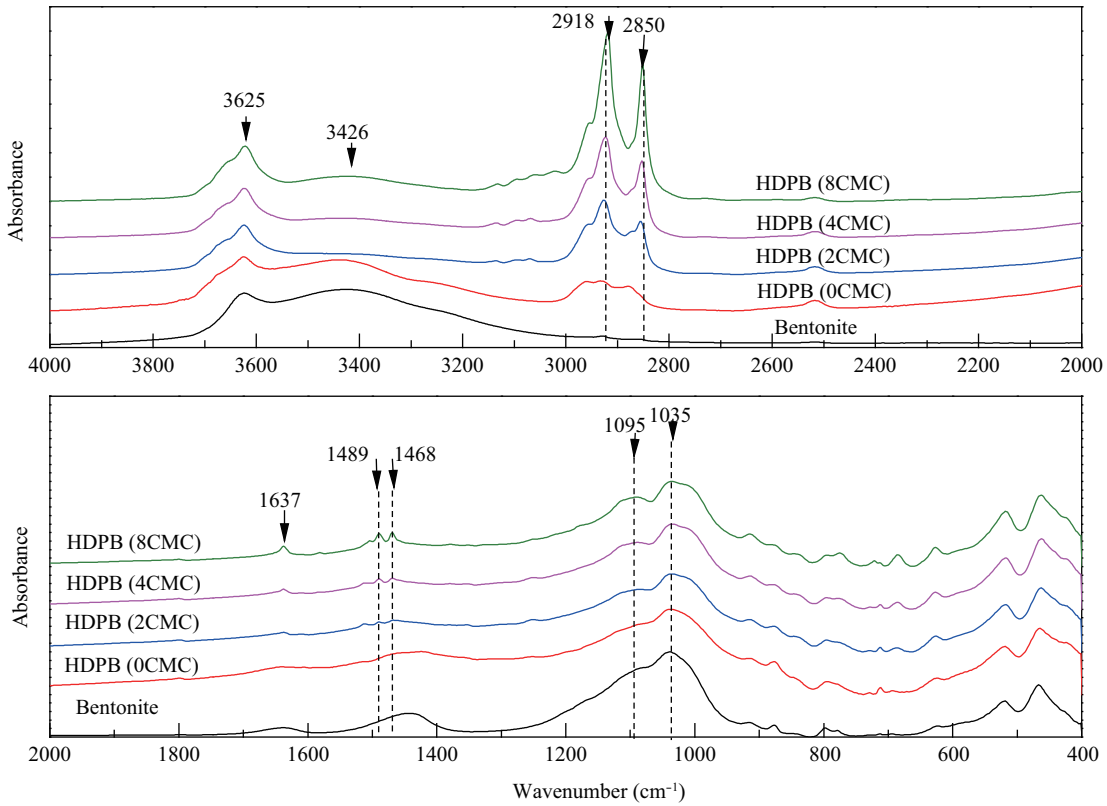

Fig. 6 FT-IR spectra of original bentonite, TX100/bentonite, and HDPB/TX100/bentonite.

calation of TX100 into the positively charged HDPB head groups.

Figure 6 shows that the frequencies of the CH_2 stretching bands of HDPB (2CMC) were 2922 and 2855 cm^{-1}, whereas those of HDPB (8CMC) were decreased to 2918 and 2850 cm^{-1}. The frequencies of CH_2 stretching bands decreased with an increase in HDPB concentration, indicating that the number of *gauche* conformers in the methylene chains was somewhat lower in the mixed micelles with higher cationic fraction. A higher ordering conformation with a higher HPDB fraction can be ascribed to non-ideal mixing, with the shielding effect of TX100 between HDPB head groups inducing a decrease in electrostatic repulsive interactions on the bentonite surface. The excursion of these frequencies also indicated the decreased spacing in the mixed surfactant headgroups and the increase in micelle aggregation number. Increases in micelle aggregation number were associated with changes in micelle shape from spherical to non-spherical (Scheuing and Weers, 1990).

2.4 TG-DTG/DTA

The thermal analysis (TG-DTG/DTA) patterns of original bentonite, TX100/bentonite, and HDPB/TX100/bentonite are shown in Fig. 7. Three major weight loss peaks of bentonite can be seen in Fig. 7a and b. The first and second peaks appeared at around 79 and 138.5°C due to the removal of hygroscopic and tightly adsorbed water from bentonite, respectively (del Hoyo et al., 2008). The most intense weight loss peak showed up at 715°C due to the dehydroxylation and structural breakdown of bentonite. The corresponding DTA curve in Fig. 7c showed that dehydration peaks were endothermic (↓), whereas the dehydroxylation peak was exothermic (↑). The total mass loss of pure TX100 took place at 130–450°C, which corresponded to the oxidation of organic matter.

Changes can also be observed in the surfactant/bentonite curves by presenting the thermal effects in the clay dehydration region and the oxidation of organic material. The weight loss peaks of all organobentonite curves at 200–750°C can be attributed to the oxidation of organic materials and the removal of lattice water (Tabak et al., 2010; Zhou et al., 2007). There was a slight shift in the dehydroxylation peak to a lower temperature of organobentonite, indicating the penetration of surfactant molecules into the silicate layer. Compared with pure TX100 at 287.5°C, the two higher DTG peaks at 324 and 374°C of TX100/bentonite were assigned to the mass loss of surfactant molecules in the silicate interlayer gallery, indicating the strong bond of the surfactant in the interlayer of bentonite. The weight loss of adsorbed water at around 79 and 138.5°C was annulled partially in all organobentonite cases, indicating that the adsorption of surfactants gave the bentonite surface a more hydrophobic property. As shown in the DTA curves in Fig. 7c, the oxidation of adsorbed surfactants during the heating of the sample is exothermic, including the oxidation of organic hydrogen in the range of 200–500°C and that of formed charcoal into CO_2 in the range of 400–750°C. The endothermic peaks after oxidation of TX100 and HDPB can be ascribed to insufficient oxygen to total combustion. As depicted in both DTG and DTA curves, the temperature of the HDPB/TX100/bentonite decomposition peaks was much lower with an increase in HDPB fraction and peak intensi-

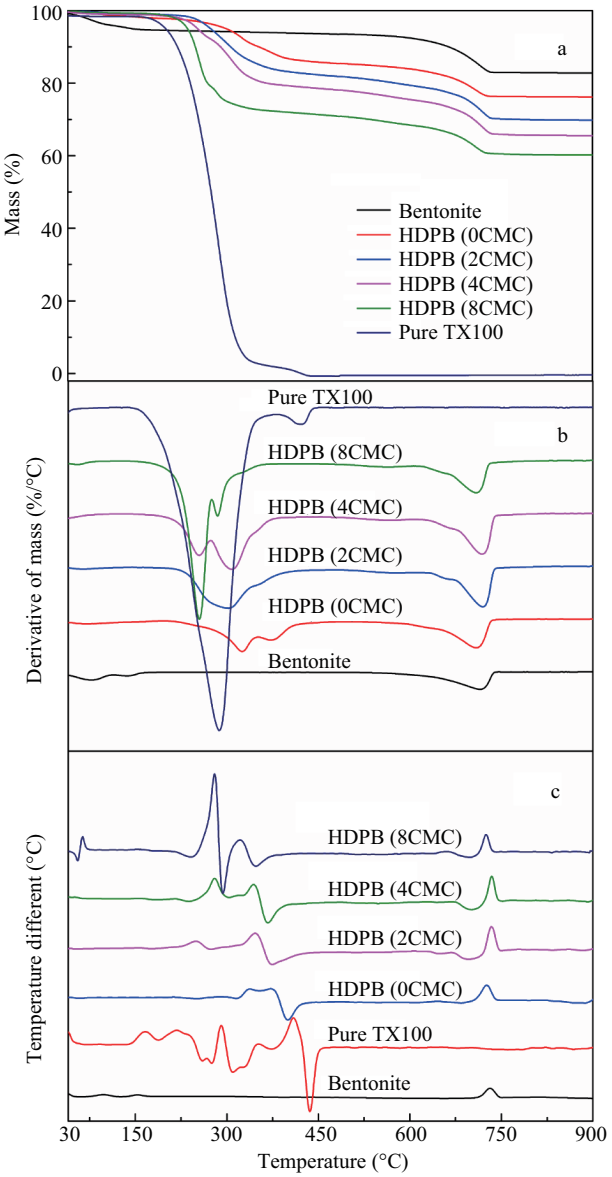

Fig. 7 TG-DTG/DTA patterns of original bentonite, HDPB/TX100/bentonite, and pure TX100.

ty. This result indicates that the conformational changes in the co-adsorption of cationic and nonionic surfactants and the higher loading of mixed surfactants onto clay mineral may reduce the thermal stability of organobentonite.

3 Conclusions

The mixed cationic-nonionic surfactants (HDPB/TX100) were adsorbed by bentonite. The cationic surfactant improved the adsorption of TX100 and total adsorbed amount significantly, indicating the good synergistic effect between HDPB and TX100. This result is mainly attributed to the pre-adsorbed HDPB molecules that acted as anchors on the bentonite surface, allowing the adsorbed HDPB to form mixed aggregates with TX100 through chain-chain interactions and promotion of TX100 adsorption.

As calculated by the nitrogen adsorption-desorption isotherms of organobentonite, the intercalation of mixed surfactants decreased the specific surface area and the total pore volume of bentonite, whereas the average pore size was increased slightly. The adsorption of surfactants generally decreased the fractal dimension (D); however, the co-adsorption of mixed surfactants resulted in a slightly higher D value. The utilization of FT-IR allowed for the determination of the conformation of the intercalated surfactants on clay mineral. The addition of HDPB increased the ordering of methylene chains on bentonite significantly. Moreover, as demonstrated by TG-DTG/DTA analysis, the thermal stability of organobentonite decreased as the amount of HDPB adsorbed increased.

The results achieved by this study can contribute to the further utilization of clay and clay mineral in the retention of HOCs and other pollutants, as well as the selection of surfactants in this process.

Acknowledgment

This work was supported by the National Natural Science Foundation of China (No. 40972151) and the National Hi-Tech Research and Development Program (863) of China (No. 2009AA064001).

References

Alkaram U F, Mukhlis A A, Al-Dujaili A H, 2009. The removal of phenol from aqueous solutions by adsorption using surfactant-modified bentonite and kaolinite. *Journal of Hazardous Materials*, 169(1-3): 324–332.

Chang Y, Lv X Q, Zha F, Wang Y G, Lei Z Q, 2009. Sorption of *p*-nitrophenol by anion-cation modified palygorskite. *Journal of Hazardous Materials*, 168(2-3): 826–831.

Chu W, So W S, 2001. Modeling the two stages of surfactant-aided soil washing. *Water Research*, 35(3): 761–767.

del Hoyo C, Dorado C, Rodriguez-Cruz M S, Sanchez-Martin M J, 2008. Physico-chemical study of selected surfactant-clay mineral systems. *Journal of Thermal Analysis and Calorimetry*, 94(1): 227–234.

Erdem B, Özcan A S, Özcan A, 2010. Preparation of HDTMA-bentonite: Characterization studies and its adsorption behavior toward dibenzofuran. *Surface and Interface Analysis*, 42(6-7): 1351–1356.

Giles C H, Macewan T H, Nakhwa S N, Smith D, 1960. Studies in Adsorption .11. A system of classification of solution adsorption isotherms, and its use in diagnosis of adsorption mechanisms and in measurement of specific surface areas of solids. *Journal of the Chemical Society*, 3973–3993.

Juang L C, Lee C K, Wang C C, Hung S H, Lyu M D, 2008. Adsorptive removal of Acid Red 1 from aqueous solution with surfactant modified titanate nanotubes. *Environmental Engineering Science*, 25(4): 519–528.

Koyuncu H, Yildiz N, Salgin U, Köroğlu F, Çalimli A, 2011. Adsorption of *o*-, *m*- and *p*-nitrophenols onto organically modified bentonites. *Journal of Hazardous Materials*, 185(2-3): 1332–1339.

Laha S, Tansel B, Ussawarujikulchai A, 2009. Surfactant-soil interactions during surfactant-amended remediation of contaminated soils by hydrophobic organic compounds: A review. *Journal of Environmental Management*, 90(1): 95–100.

Liu Z B, Edwards D A, Luthy R G, 1992. Sorption of nonionic surfactants onto soil. *Water Research*, 26(10): 1337–1345.

Ninness B J, Bousfield D W, Tripp C P, 2002. The importance

of adsorbed cationic surfactant structure in dictating the subsequent interaction of anionic surfactants and polyelectrolytes with pigment surfaces. *Colloids and Surfaces A-Physicochemical and Engineering Aspects*, 203(1-3): 21–36.

Portet-Koltalo F, Desbène P L, Treiner C, 2001. Self-desorption of mixtures of anionic and nonionic surfactants from a silica/water interface. *Langmuir*, 17(13): 3858–3862.

Rodríguez-Cruz M S, Andrades M S, Sánchez-Martín M J, 2008. Significance of the long-chain organic cation structure in the sorption of the penconazole and metalaxyl fungicides by organo clays. *Journal of Hazardous Materials*, 160(1): 200–207.

Rodríguez-Cruz M S, Sánchez-Martín M J, Andrades M S, Sánchez-Camazano M, 2007. Modification of clay barriers with a cationic surfactant to improve the retention of pesticides in soils. *Journal of Hazardous Materials*, 139(14): 363–372.

Sánchez-Martín M J, Dorado M C, del Hoyo C, Rodríguez-Cruz M S, 2008. Influence of clay mineral structure and surfactant nature on the adsorption capacity of surfactants by clays. *Journal of Hazardous Materials*, 150(1): 115–123.

Scheuing D R, Weers J G, 1990. A Fourier-Transform Infrared spectroscopic study of dodecyltrimethylammonium chloride sodium dodecyl-sulfate surfactant mixtures. *Langmuir*, 6(3): 665–671.

Sehgal P, Kosaka O, Doe H, Otzen D E, 2009. Interaction and stability of mixed micelle and monolayer of nonionic and cationic surfactant mixtures. *Journal of Dispersion Science and Technology*, 30(7): 1050–1058.

Senturk H B, Ozdes D, Gundogdu A, Duran C, Soylak M, 2009. Removal of phenol from aqueous solutions by adsorption onto organomodified Tirebolu bentonite: Equilibrium, kinetic and thermodynamic study. *Journal of Hazardous Materials*, 172(1): 353–362.

Shu Y H, Li L S, Zhang Q Y, Wu H H, 2010. Equilibrium, kinetics and thermodynamic studies for sorption of chlorobenzenes on CTMAB modified bentonite and kaolinite. *Journal of Hazardous Materials*, 173(1-3): 47–53.

Sing K S W, Everett D H, Haul R A W, Moscou L, Pierotti R A, Rouquerol J et al., 1985. Reporting physisorption data for gas solid systems with special reference to the determination of surface-area and porosity (Recommendations 1984). *Pure and Applied Chemistry*, 57(4): 603–619.

Singhal R, Datta M, 2007. Development of nanocomposites of bentonite with polyaniline and poly(methacrylic acid). *Journal of Applied Polymer Science*, 103(5): 3299–3306.

Somasundaran P, Huang L, 2000. Adsorption/aggregation of surfactants and their mixtures at solid-liquid interfaces. *Advances in Colloid and Interface Science*, 88(1-2): 179–208.

Tabak A, Baltas N, Afsin B, Emirik M, Caglar B, Eren E, 2010. Adsorption of Reactive Red 120 from aqueous solutions by cetylpyridinium-bentonite. *Journal of Chemical Technology and Biotechnology*, 85(9): 1199–1207.

Thibaut A, Misselyn-Bauduin A M, Grandjean J, Broze G, Jèrome R, 2000. Adsorption of an aqueous mixture of surfactants on silica. *Langmuir*, 16(24): 9192–9198.

Torn L H, de Keizer A, Koopal L K, Lyklema J, 2003. Mixed adsorption of poly(vinylpyrrolidone) and sodium dodecylbenzenesulfonate on kaolinite. *Journal of Colloid and Interface Science*, 260(1): 1–8.

Varade D, Bahadur P, 2005. Interaction in mixed micellization of sodium N-tetradecanoylsarcosinate with ionic and nonionic surfactants. *Journal of Dispersion Science and Technology*, 26(5): 549–554.

Wang C C, Juang L C, Lee C K, Hsu T C, Lee J F, Chao H P, 2004. Effects of exchanged surfactant cations on the pore structure and adsorption characteristics of montmorillonite. *Journal of Colloid and Interface Science*, 280(1): 27–35.

Wang T, Zhu J X, Zhu R L, Ge F, Yuan P, He H P, 2010. Enhancing the sorption capacity of CTMA-bentonite by simultaneous intercalation of cationic polyacrylamide. *Journal of Hazardous Materials*, 178(1-3): 1078–1084.

Xi,Y F, Mallavarapu M, Naidu R, 2010. Preparation, characterization of surfactants modified clay minerals and nitrate adsorption. *Applied Clay Science*, 48(1-2): 92–96.

Xu S H, Boyd S A, 1995. Cationic surfactant adsorption by swelling and nonswelling layer silicates. *Langmuir*, 11(7): 2508–2514.

Zhang L, Somasundaran P, 2006. Adsorption of mixtures of nonionic sugar-based surfactants with other surfactants at solid/liquid interfaces I. Adsorption of *n*-dodecyl-beta-D-maltoside with anionic sodium dodecyl sulfate on alumina. *Journal of Colloid and Interface Science*, 302(1): 20–24.

Zhao Q, Yang K, Li P J, 2010. Enhanced soil retention for o-nitroaniline by the addition of a mixture of a cationic surfactant (Cetyl Pyridinium Chloride) and a nonionic surfactant (Polyethylene Glycol Mono-4-nonylphenyl Ether). *Journal of Hazardous Materials*, 182(1-3): 757–762.

Zheng Z M, Obbard J P, 2002. Evaluation of an elevated non-ionic surfactant critical micelle concentration in a soil/aqueous system. *Water Research*, 36(10): 2667–2672.

Zhou Q, Frost R L, He H P, Xi Y F, 2007. Changes in the surfaces of adsorbed para-nitrophenol on HDTMA organoclay- The XRD and TG study. *Journal of Colloid and Interface Science*, 307(1): 50–55.

Zhou W J, Zhu L Z, 2005. Distribution of polycyclic aromatic hydrocarbons in soil-water system containing a nonionic surfactant. *Chemosphere*, 60(9): 1237–1245.

Zhu J, Zhu L Z, Zhu R L, Tian S L, Li J W, 2009. Surface microtopography of surfactant modified montmorillonite. *Applied Clay Science*, 45(1-2): 70–75.

JOURNAL OF ENVIRONMENTAL SCIENCES

Journal of Environmental Sciences (Established in 1989)
Vol. 24 No. 8 2012

Supervised by	Chinese Academy of Sciences	**Published by**	Science Press, Beijing, China
Sponsored by	Research Center for Eco-Environmental Sciences, Chinese Academy of Sciences		Elsevier Limited, The Netherlands
		Distributed by	
Edited by	Editorial Office of Journal of Environmental Sciences (JES) P. O. Box 2871, Beijing 100085, China Tel: 86-10-62920553; http://www.jesc.ac.cn E-mail: jesc@263.net, jesc@rcees.ac.cn	Domestic	Science Press, 16 Donghuangchenggen North Street, Beijing 100717, China Local Post Offices through China
		Foreign	Elsevier Limited http://www.elsevier.com/locate/jes
Editor-in-chief	Hongxiao Tang	**Printed by**	Beijing Beilin Printing House, 100083, China

CN 11-2629/X **Domestic postcode: 2-580** **Domestic price per issue RMB ¥ 110.00**

ISSN 1001-0742